Dependable Open-Phase Detection for Inverter-Based Energy Resources

Brett Cockerham and Joseph Miller
Burns & McDonnell

Jai Subbarayan and Abd-Ahmed Elkader
Schweitzer Engineering Laboratories, Inc.

Presented at the
79th Annual Georgia Tech Protective Relaying Conference
Atlanta, Georgia
April 15–17, 2026

Originally presented at the
78th Annual Conference for Protective Relay Engineers, March 2025

Dependable Open-Phase Detection for Inverter-Based Energy Resources

Brett Cockerham and Joseph Miller, *Burns & McDonnell*
Jai Subbarayan and Abd-Ahmed Elkader, *Schweitzer Engineering Laboratories, Inc*.

***Abstract*—Integrating inverter-based distributed energy resources (DERs) into distribution systems has yielded operational concerns and challenges. One of these challenges is to reliably detect an open phase at the interconnection point. Conventional methods of open-phase detection are optimized for power systems with rotating machine sources and hence struggle to maintain reliability when applied at inverter-based DER interconnection points. Additionally, the presence of some types of interconnection transformers can impose additional challenges to open-phase detection.**

In this paper, we introduce a current-based open-phase detection method designed to maintain reliability when the DER is an inverter-based source. This method detects an open phase when there is sufficient current flowing between the inverter-based DER and the area electric power system (EPS). The absence of current on the disconnected phase—while current continues to flow on the connected phases—combined with supervisory conditions, is used to detect the open phase. The technical paper, "Field Experience With Open-phase Testing at Sites With Inverter-Based Resources," established voltage-based open-phase detection methods. These voltage-based open-phase detection methods are employed to maintain reliability when there is insufficient current flowing between the inverter-based DER and the area EPS.

We use field events to demonstrate the overall reliability of combining the previously employed voltage-based open-phase detection scheme and the proposed current-based open-phase detection scheme at the interconnection point for inverter-based DER applications. Furthermore, we use real-time digital simulator (RTDS) to demonstrate the reliability of the proposed current-based open-phase detection scheme.

I. Introduction

Open-phase conditions may result in overvoltages that can exceed ratings and result in equipment damage. Open-phase conditions may also result in excessive harmonics on both the local-system voltage and the current injected into the system by the inverter-based DER [1]. Failure of an inverter-based DER to trip offline and cease energization within two seconds after an open-phase condition—at the point of common coupling (PCC)—will result in non-compliance with IEEE 1547-2018 [2]. Non-compliance with the inverter-based DER with open-phase requirements of IEEE 1547-2018 may result in the delay of plant commissioning [3].

IEEE 1547.1-2020 outlines a type test to confirm the isolation of the inverter-based DER following an open-phase condition. This test includes opening one phase-disconnect switch when the DER is outputting the maximum of either five percent of the rated DER output current or the minimum output current rating of the DER [4]. The DER must trip offline and cease energization within the timeframe specified by IEEE 1547-2018.

The PCC is typically located on the high-voltage side of the step-up transformer. Current transformers (CTs) and potential transformers (PTs) are typically installed at the PCC, as shown in Fig. 1. The current and voltage measurements from the CTs and PTs are used in the protection schemes at the PCC. The current level output of inverter-based DERs—such as photovoltaics and wind turbines—is tied to the amount of solar irradiance and wind speed, respectively. As a result, traditional open-phase detection (OPD) algorithms based on current measurements may not see enough current to securely declare an open-phase condition present during low or no-load operation of the inverter-based DER. In some cases, the winding connections and core construction of the step-up transformer may allow the voltage on the lost phase to be partially reconstructed, negatively impacting the dependability of commonly applied phase undervoltage protection to respond to an open-phase condition [5]. To overcome these complications, protection methods based on zero-sequence voltage and total harmonic distortion of voltage were proposed in [1] and are reviewed in Section II. The voltage-based methods offer dependable operation during low current output by the DER.

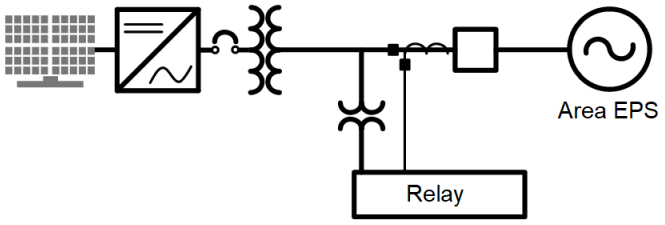

Fig. 1. CT and PT at the PCC

When the DER is outputting sufficient current, alternatives to the voltage-based detection scheme may provide improved dependability. The need for current-based OPD is further illustrated in Section III. A review of existing current-based schemes is presented in Section IV. That these schemes rely on sequence currents (I2/I1 and I0) is unfavorable due to the unpredictability of negative-sequence currents near inverter-based DERs. Furthermore, sequence current-based schemes are prone to operate for asymmetrical shunt faults. To improve the selectivity of current-based OPD, this paper presents a protection algorithm relying on fundamental current measurements taken at the PCC, as shown in Section V.

Combining voltage- and current-based methods enhances the dependability of OPD. The combined OPD protection

algorithm is tested with field events and RTDS simulations in Sections VI and VII, respectively, to demonstrate improved dependability.

II. Voltage-Based OPD

Two voltage-based OPD schemes documented in [1] have been widely applied across the industry in applications involving inverter-based DERs. These two voltage-based schemes use the measured zero-sequence voltage and total harmonic distortion to provide increased dependability for OPD during times of insufficient wind or low solar irradiance when compared against typical current-based OPD schemes. There is a common logic between the two schemes that secures the elements during transformer energization, faults, switching, and VT fuse failure. The output of this securing logic is shown in Fig. 2.

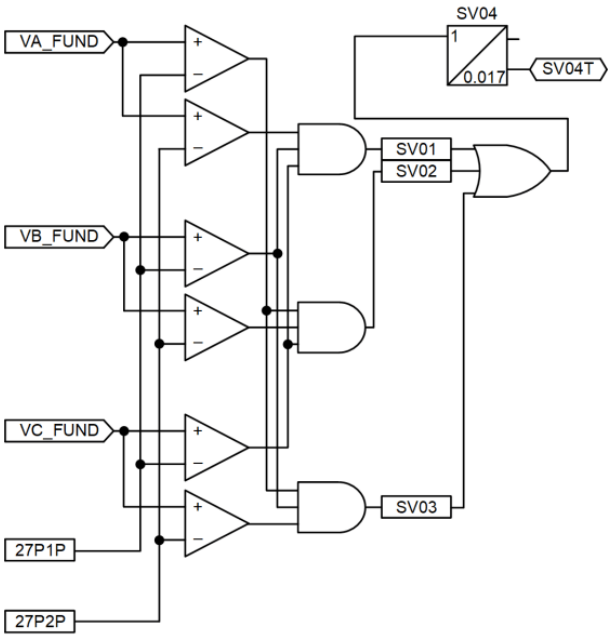

Fig. 2. Undervoltage Securing Logic

Note that the time qualifiers for the schemes detailed in [1] are specified using cycles. In this paper, all time qualifiers are specified in seconds as those were the units implemented in the user settings of the OPD device.

The securing logic in Fig. 2 assumes that the PTs are connected to the transformer side of the PCC breaker, as shown in Fig. 1. If the PTs used for this scheme are installed on the EPS side of the PCC, then a slight modification to the logic is needed to add 52A supervision [1].

The output of the zero-sequence overvoltage scheme (SV05T), in Fig. 3, capitalizes on the voltage unbalance that generally occurs when an open-phase condition exists. For security, this scheme is only active when the inverter-based DER is exporting low or no power and is therefore supervised by the absence of phase current (50LP) and zero-sequence current (50GP). To prevent the scheme from operating for shunt faults, the 50GP may be set less than the PCC relay pickup setting, specified to operate for ground faults. 50LP will be used as a common threshold setting with the proposed current-based OPD scheme. Guidance in specifying this threshold is reviewed later in Section V. The 50LP multiplier of two ensures that there will be overlapping protection of the zero-sequence overvoltage scheme and the proposed current-based OPD scheme.

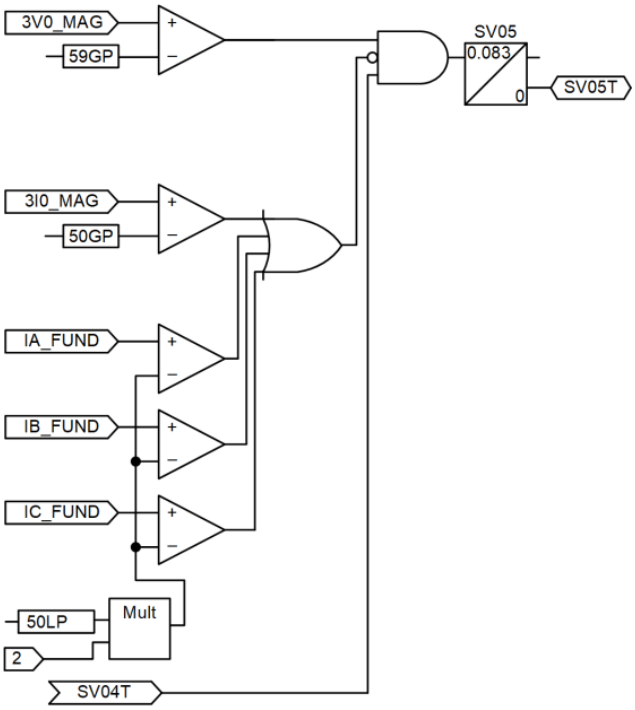

Fig. 3. Zero-Sequence Overvoltage Scheme

A sudden increase in voltage total harmonic distortion (V-THD) may be observed on the measured phase in which the open-phase condition exists [1]. In these cases, the V-THD scheme yields dependable results. The logic for the V-THD scheme (SV06T) is illustrated in Fig. 4.

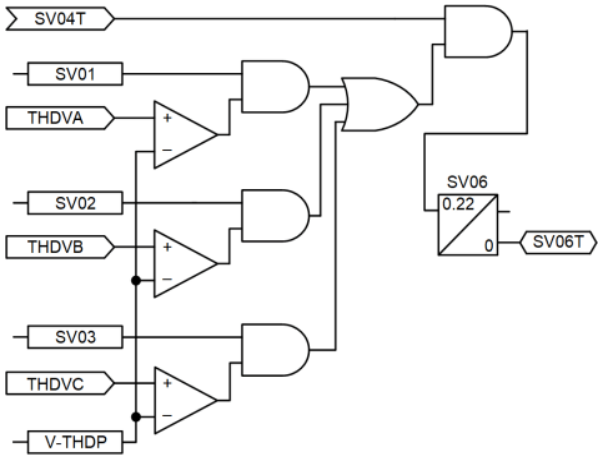

Fig. 4. Voltage THD Scheme

III. Need For Current-Based OPD

When the inverter-based DER is exporting low or no power to the area EPS, both the zero-sequence overvoltage scheme and the V-THD scheme are available to detect an open phase. When more current is flowing through the PCC, the zero-sequence overvoltage scheme gets blocked, as shown in Fig. 3, while the V-THD scheme remains available.

As shown in [1] and later in Table II, the V-THD scheme is not 100 percent effective in detecting an open phase. The level of voltage harmonic distortion during an open phase depends on conditions such as the severity of ferroresonance at the PCC and the inverter output current. These conditions are difficult to predict or model, thereby increasing the complexity of application.

To improve the dependability of OPD under significant current flow at the PCC, a separate method that is easy to test and apply is needed. For this, a current-based OPD scheme is proposed in this paper.

IV. Existing Current-Based OPD

Several methods based on currents have been implemented in microprocessor relays to detect an open phase on the area EPS side of the interconnecting transformer. These methods require careful consideration of various application parameters, such as the transformer connection type and presence of grounding transformers. Furthermore, these methods generally require extensive testing and validation from system models to maintain security during shunt faults. We review some of these methods in this section.

A. Sequence Current Ratio Methods

A conventional method for detecting open-phase on radial feeders is to use the ratio of negative-sequence current to the positive-sequence current (I2/I1) [6]. In this method, the series fault (open-phase) is modeled to exist in a radial part of the system, with a balanced three-phase source and three-phase loads. The expected I2 resulting from the unbalance created by the open phase can be estimated and used as the basis for setting the OPD scheme with I2/I1 as the operating quantity. The I2/I1 method has also been used to detect open-phase faults that occur upstream of power delivery transformers, wherein the transformer winding connections must be modeled to properly estimate the expected I2/I1 on the primary side of a transformer [5].

This paper focuses on OPD at the interconnection point to inverter-based DER. These unconventional sources do not inject reliable negative-sequence currents during fault conditions, which makes I2/I1 unreliable for use in such applications [7]. In applications where a ground current source is present on the primary side of the interconnection transformer—such as in cases where the transformer is wye-grounded primary and delta secondary—the zero-sequence current magnitude can be used to detect an open phase on the wye side of the transformer [8]. However, such a method would require restraint or time coordination with 51/50G protection during utility-side ground faults, where significant 3I0 could flow through the DER transformer.

B. Reference Signal-Based Detection

A sensitive current-based scheme was developed to detect an open phase on the high side of station auxiliary transformers at nuclear power plants. Three different algorithms are proposed in this scheme. In one algorithm, the transformer excitation current is measured at no load and averaged over time. If any phase current drops below this value, an open phase is declared. Another algorithm passes the measured phase current through an infinite impulse response (IIR) filter and compares the output of this filter to the instantaneous phase current magnitude. A drop in phase current below a percentage of the IIR filter output is used to detect the open phase. Finally, another algorithm measures the incremental change in the ratio of second harmonic to the fundamental component of the phase current and counts the number of times this incremental change exceeds a minimum threshold. This count is expected to increase quickly following an open phase and subsequently, to be detected by this algorithm [9]. In some cases, this scheme allows the open-phase fault to be detected even at light-loading or no-load conditions.

However, this method requires advanced relay features that are not typically available at DER installations.

C. Active Neutral Signal Injection-Based Detection

Another method developed for nuclear plant station service transformers uses a non-harmonic (between 45-90 Hz) voltage signal that is coupled to the transformer wye-grounded high-side winding neutral using a CT. An electronic controller measures the neutral current (the injected current in the neutral) to calculate impedance against the injected signal. This calculation normally measures the combined zero-sequence impedance of the transformer and the system, and tracks the change in impedance during an open phase for detection [10].

However, this method requires dedicated hardware for OPD, which is typically not available at DER installations. Furthermore, this method is applicable only in cases where the high side winding is wye-grounded.

V. Proposed Current-Based OPD Method

As reviewed, many of the existing current-based OPD methods may also operate for shunt faults, thus challenging the selectivity of the protection scheme and introducing coordination challenges. Alternatively, some solutions require specialized equipment, which is rarely considered. This proposed current-based OPD can be programmed in off-the-shelf digital relays or power quality meters. Additionally, the scheme can be applied independently of the transformer connection type and provides increased selectivity over traditional methods. The proposed scheme consists of the arming logic illustrated in Fig 5.

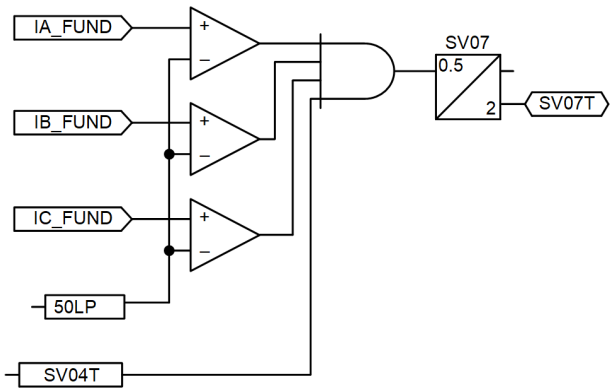

Fig 5. Arming Logic

Some devices available on the market today allow the user to build custom logic using rms analogs and/or fundamental analogs; however, most digital protection relays used in the industry use a digital filter to extract the fundamental component of the signal, which is then applied as the operating quantity for protection. Therefore the scheme illustrated in this paper uses fundamental currents. Rms analogs may substitute for fundamental currents when available. Additional details when considering rms analogs are provided in Section VIII.

The arming logic ensures there is a measurable amount of fundamental current IA_FUND, IB_FUND, and IC_FUND (i.e., 50 Hz or 60 Hz) on all three phases for the duration specified in setting SV07PU (i.e., 0.5 seconds).

Additionally, the arming logic uses the same 50LP setting threshold and undervoltage securing logic (SV04T) as described previously. For added security, the SV07DO timer user setting specifies the duration in which the scheme will remain active following a loss in phase current or voltage. One of the requirements imposed by IEEE 1547-2018 is to detect and trip all phases within two seconds for any open-phase condition and, therefore, two seconds was selected for SV07DO [2].

The SV07T arming logic supervises the output of the proposed current-based OPD scheme (SV15) illustrated in Fig. 6. This scheme operates when a loss of current is observed on a single phase while current is still measured on the two other remaining phases.

When the measured current on two phases exceeds 50LP, but the measured current on a single phase drops below 0.8 • 50LP, the open-phase logic for the phase with diminished current asserts (SV12T, SV13T, and SV14T).

Selecting the 50LP threshold is dependent on several factors, such as DER-rated output, current transformer ratio (CTR), and the OPD device (i.e, protective relay or programmable meter) measuring range. Equation (1) can be used as the setting basis for selecting the measured current threshold 50LP in amperes secondary:

$$50LP = 0.7 \bullet k \bullet \frac{MVA \bullet 1000}{kV \bullet CTR \bullet \sqrt{3}} \qquad (1)$$

where:

k is the maximum of either one the following:

1. 5 percent of the rated inverter-based DER output current
2. The minimum output current rating of the DER.

MVA is the DER-rated output power, in MVA

kV is the line-to-line voltage at the PCC, in kV

CTR is the effective current transformer ratio wired to the OPD device

Proper CTR is paramount to ensure the current-based OPD scheme is reliable, as (1) may yield a threshold below the measurable range of the OPD device. Reference [11] provides insight for sizing the CTR in a protection application where increased sensitivity is needed.

Care should be taken in determining the pickup time qualifiers SV12PU, SV13PU, and SV14PU. The calculation window for the analogs may vary depending on the device in which the logic is applied. In the device used for developing these schemes, the fundamental currents are calculated using a one-cycle cosine filter and the update rates defined by the device for these analogs are once every half-cycle. For added security, the pickup time chosen for this scheme is 0.03 seconds. This ensured that at least four consecutive 1/2-cycle measurements satisfied the logic conditions to declare an open-phase event. The initial measurement that drives the SV12, SV13, and SV14 logic to a logical TRUE condition and then the following three updates must remain true to assert the logic, as it is supervised by the pickup timer. Too long of a pickup time may result in the inverter shutting down and the phase currents going to zero prior to the operation of the OPD scheme. Furthermore, the fast action of the scheme may limit the duration of overvoltages on equipment. The logical OR combination of the voltage-based schemes and proposed current-based scheme is illustrated in Fig. 7. Additionally, a comprehensive table for setting recommendations is provided in the Appendix. These guidelines can be used as a basis when combining both current- and voltage-based schemes, as illustrated in Fig. 7.

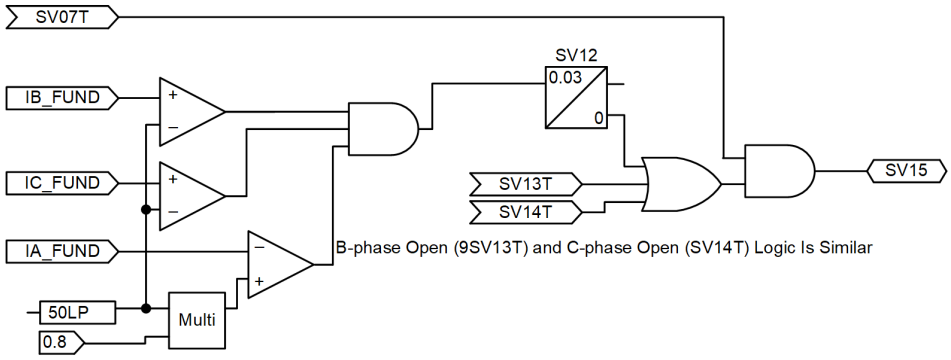

Fig. 6. Fundamental Current-Based OPD Scheme

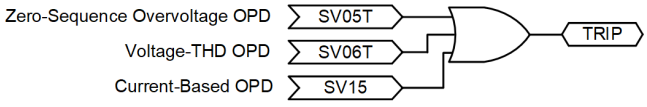

Fig. 7. OPD Trip Logic

VI. Analysis of Field Events

Event data were collected during commissioning tests from several inverter-based DER installations at different locations across the United States. A selection of these events were previously presented in [1] to develop the voltage-based OPD method reviewed in Section II. This paper replays the discussed event reports from five different sites to demonstrate the performance of the proposed current-based OPD method. Sites 1, 2, and 5 were presented in [1]. Sites 3 and 4 are new to this paper.

Fig. 8 displays a generic single-line representation of the systems in which the commissioning tests were performed.

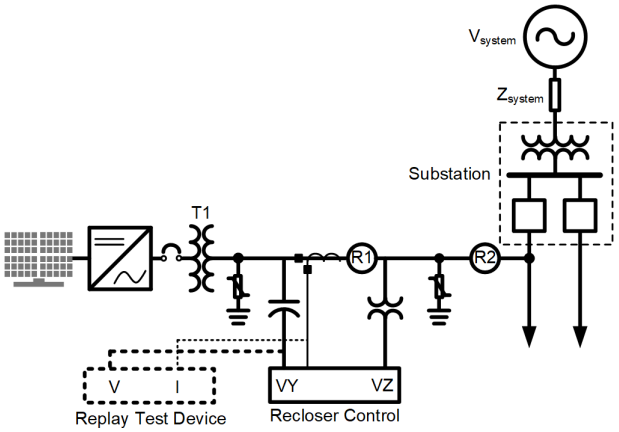

Fig. 8. DER Interconnection Topology Example

These applications include two pole-top reclosers (R1 and R2) in series at the PCC. The recloser controller that is connected to each recloser, is a microprocessor-based relay with three-phase voltage measurement capability on both the utility and the DER side of the recloser (six voltage inputs total). Note that the utility-side voltages are measured with a wire-wound PT and the DER-side voltages are measured using low-energy analog sensors with capacitive voltage dividers installed in the recloser bushings.

To demonstrate compliance with the open-phase type test requirements of IEEE 1547.1-2020, the utility initiated a single-phase trip at R2. The resulting event data were recorded by the recloser control at R1. In some of the field events captured, R1 is already programmed with a version of the voltage-based OPD scheme, as discussed in [1]. In these field cases, the OPD was properly detected and the PCC tripped accordingly. However, to evaluate the performance of the proposed current-based OPD scheme, the currents and the DER-side voltages captured in these events were replayed in the OPD device, which was programmed with the proposed OPD method. A common CT ratio of 200:5 was selected. PT ratios were selected such that a nominal secondary line-to-neutral voltage of 120 V was available at the OPD device. 50LP is set to 0.2 amperes secondary in this analysis.

Table I details the CTR and potential transformer ratio (PTR) for the replay testing, the transformer connection, DER-rated output, rated voltage levels, the number of inverters tied to the collector bus, and the load flow level at the PCC as a percentage of the of the full capacity of the inverter for each of the five sites.

TABLE I
System Data for Open-Phase Replay Testing Cases

	Site 1	Site 2	Site 3	Site 4	Site 5
OPD Device CTR	200:5				
OPD Device PTR	66:1	110:1	110:1	64:1	120:1
Vector Group	YNy0	YNy0	YNy0	YNy0	YNy0
DER-Rated AC Output (MW)	5	5	5	2	7.5
Nominal High Voltage (kV)	12.47	22.86	22.86	13.2	23.9
Nominal Low Voltage (V)	600	575	550	480	600
Total Inverter Count	2	3	2	33	3
Load Level (% of Capacity)	17.71%	86.39%	25.96%	86.26%	51.33%

Events generated from the replay testing are presented in this section. The magnitude of the fundamental component of the voltages is labeled as Vp_FUND (p = A, B, C) and the currents are labeled as Ip_FUND (p = A, B, C). The raw voltage waveforms are labeled as Vp (p = A, B, C) and the currents are labeled as Ip (p = A, B, C). The fundamental values are calculated by the OPD device as described in Section IV. The voltage and current analogs are shown in primary values. Thresholds 50LP and 50LP•0.8 are also reflected in primary values for comparison.

A. Site 1

Fig. 9 shows an open phase on Phase C. As mentioned before, this is created by opening a pole on the R2 recloser.

The Ip_FUND values show that before the open phase occurred, the filtered current magnitudes on all three phases were higher than the yellow line (50LP_THRES).This allows the current-based OPD scheme to be armed (SV07T, refer to logic diagram in Fig 5.

As the open phase occurs, Phase C current magnitude (IC_FUND) drops below the magenta line (NOT_50LP_THRES), while IA_FUND and IB_FUND remain above the yellow line (50LP_THRES). This characteristic response is detected (SV14) by the current-based OPD logic shown in Fig. 6. And an OPD trip (SV15) is issued by the OPD device within 0.05 seconds of open-phase inception.

Recloser control R1 is tripped about 0.140 seconds into the fault by the onboard voltage-based OPD scheme. Reference [1] examines the same event in more detail to explain the decision made by R1 during this commissioning test.

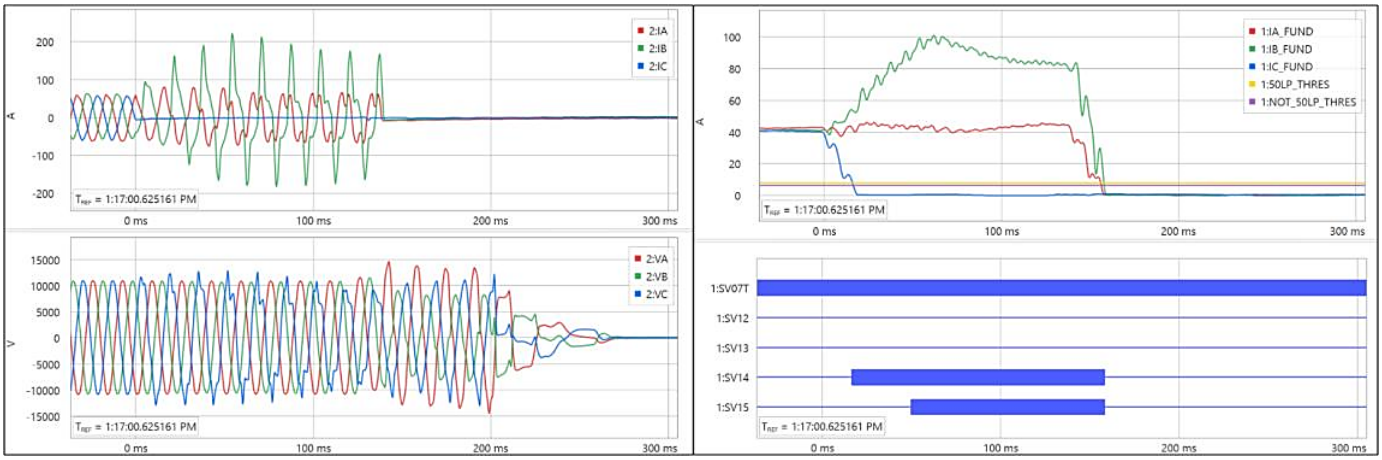

Fig. 9. Site 1 Replay Test Event Report

B. Site 2

Fig. 10 shows an open phase on Phase A. Following this, noticeable spikes in current are observed on Phase A. These spikes are aligned with voltage peaks on that phase and attributed to arrester(s) conduction due to the high instantaneous voltage. The instantaneous voltage observed during this event was excessive and could lead to arrester failure, insulation failure, or evolve to high-current faults if not detected and cleared quickly. The spikes in the current persisted until the DER was removed from the system.

In the top-right plot in Fig. 10, the Ip_FUND values show that before the open phase occurred, the filtered current magnitudes on all three phases were higher than the yellow line 50LP_THRES and this allows the current-based OPD scheme to be armed (SV07T). Following the open phase, the current magnitude on Phase A (IA_FUND) drops below the magenta line (NOT_50LP_THRES) momentarily, then rises above the magenta line for about 0.04 seconds before dropping back below the magenta line, while IB_FUND and IC_FUND remain above the yellow line (50LP threshold). This satisfies the current-based OPD scheme to pick up (SV12) and trip (SV15) around 0.11 seconds into the open phase. The increase in trip time is due to the presence of arrester current on the open phase

Since IA_FUND eventually drops below the magenta line in this event, the current-based OPD scheme remains dependable. In cases where arrester current is persistent and higher in magnitude, the current-based OPD scheme may fail to detect the open phase.

It was observed that the DER current output (Ip) decayed to zero around 0.116 seconds following the inception of the open phase fault as the DER overvoltage protection asserted and disconnected all three phases at the low-side ac contactor.

If the current-based OPD scheme fails to trip, the voltage-based OPD schemes are relied upon to trip the PCC breaker after the inverter-based DER output currents shut down. The zero-sequence overvoltage OPD scheme issues a trip (SV05T) after the inverter current output shuts down, as 3V0 is higher than the green line (59GP_THRES) on the bottom-right plot shown in Fig. 10.

While the V-THD scheme does not pick up (SV06) or trip (SV06T) within the scope of this event, Phase-A voltage is heavily distorted with a THD of 84.65 percent, and this scheme is expected to trip under two seconds. To confirm this supposition, this event was replayed again on the OPD device, with the last 0.2 seconds of the waveforms repeated at the tail end of the event to allow more time for the V-THD scheme to pick up. As expected, the V-THD scheme picks-up and trips 0.66 seconds after the open phase occurs.

During the commissioning test where this event was originally recorded, Recloser R1 was eventually tripped manually by onsite personnel. The event data in Fig. 10 doesn't display the signals at the time of the manual operation [1].

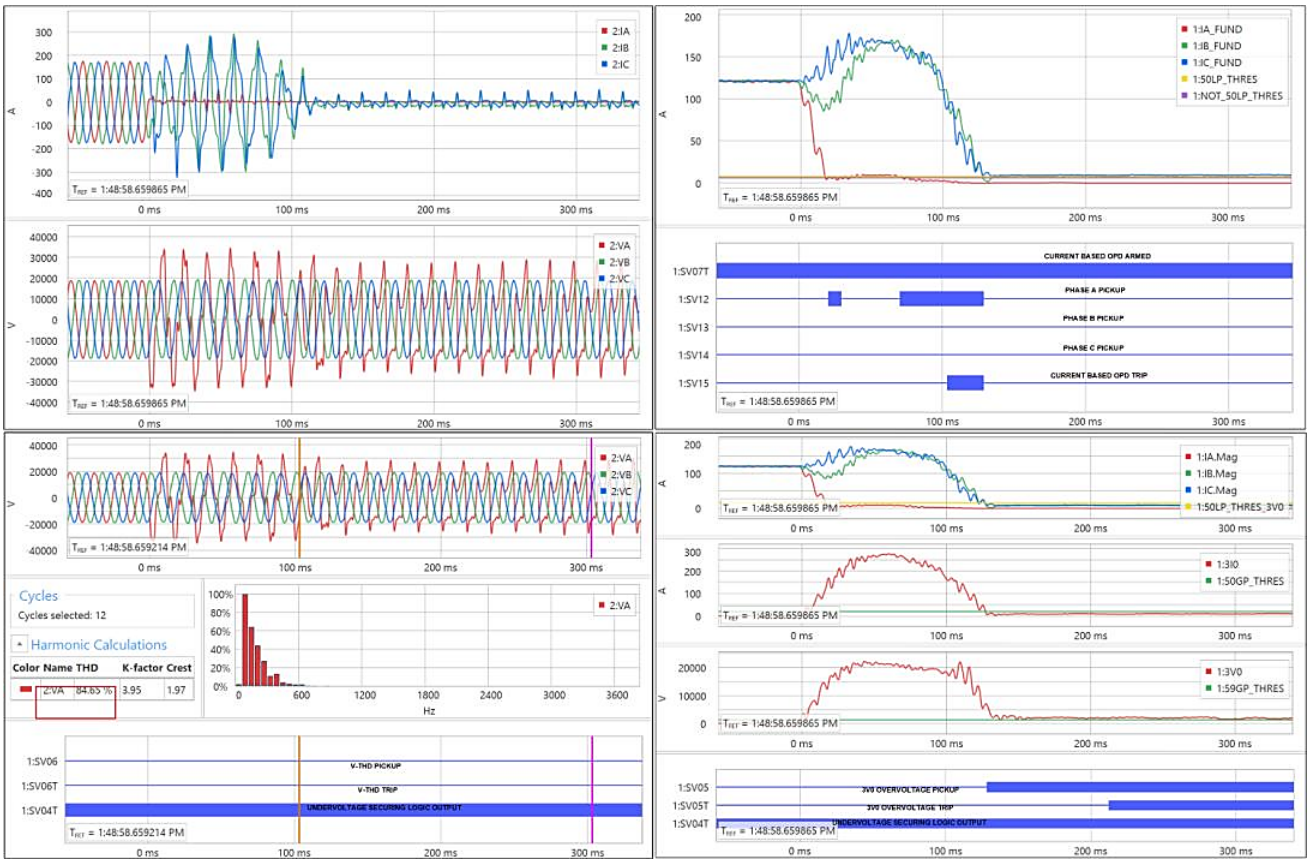

Fig. 10. Site 2 Replay Test Event Report

C. *Site 3*

Fig. 11 shows an open-phase fault on Phase A, on the system-side of PCC Recloser R1. Similar to the event reviewed in Site 1, Ip_FUND values show that before the open phase occurred, the filtered current magnitudes on all three phases were higher than the yellow line (50LP_THRES) and this allows the current-based OPD scheme to be armed (SV07T). Following the open phase, the current magnitude on Phase A (IA_FUND) drops below the magenta line (NOT_50LP_THRES), while IB_FUND and IC_FUND remain above the yellow line (50LP_THRES). This satisfies the current-based OPD scheme to pick up (SV12) and trip (SV15) in 0.044 seconds.

Recloser R1 is tripped by the onboard voltage-based OPD scheme in 0.137 seconds and the inverter-based DER output voltages collapse soon after Recloser R1 is opened.

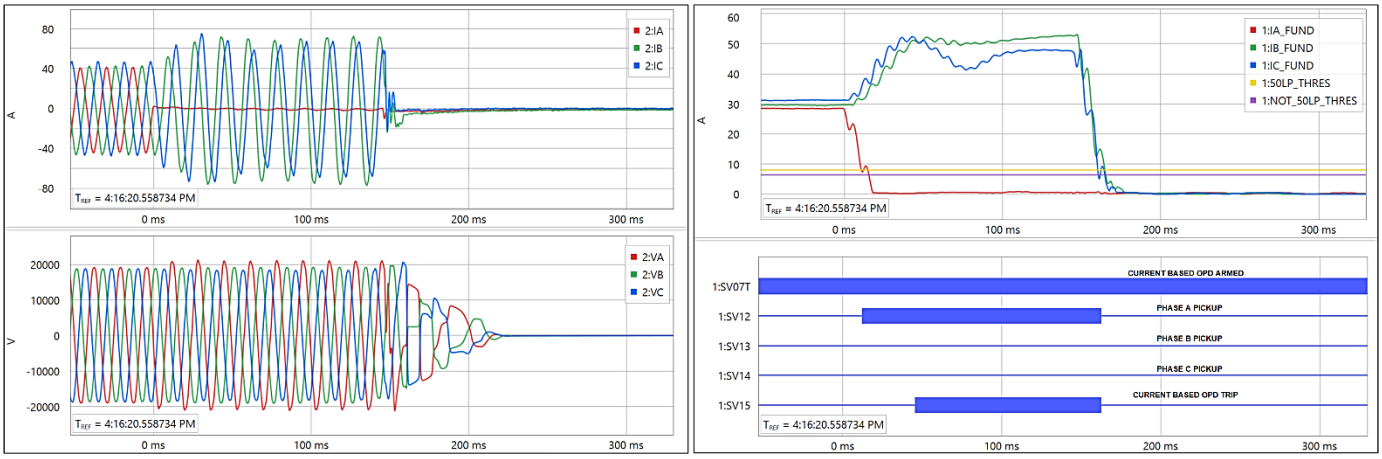

Fig. 11. Site 3 Replay Test Event Report

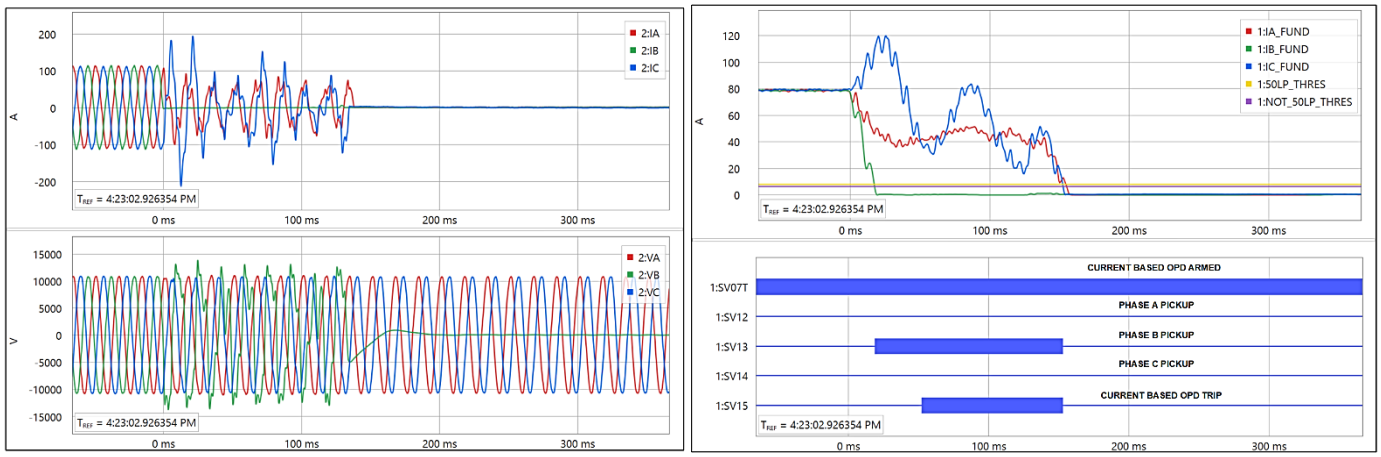

Fig. 12. Site 4 Replay Test Event Report

D. Site 4

Fig. 12 shows an open phase on Phase B, on the system side of PCC Recloser R1. The current-based OPD scheme is armed and picks up as IB_FUND drops below the magenta line (NOT_50LP_THRES), IA_FUND and IC_FUND remain above the yellow line (50LP_THRES). This satisfies the current-based OPD scheme to pick up (SV13) and trip (SV15) under 0.055 seconds.

The DER output current is heavily distorted (greater than 20 percent THD on the unfaulted phases), which causes some oscillation in the current magnitude estimation on Phase C, but it does not prevent the current-based OPD scheme from tripping. Recloser R1 trips 0.137 seconds after the open-phase fault inception. Note that the voltages were captured from the system side of the Recloser for events from this site and, therefore, nominal voltages on A-phase and C-phase are still measured until the end of the event.

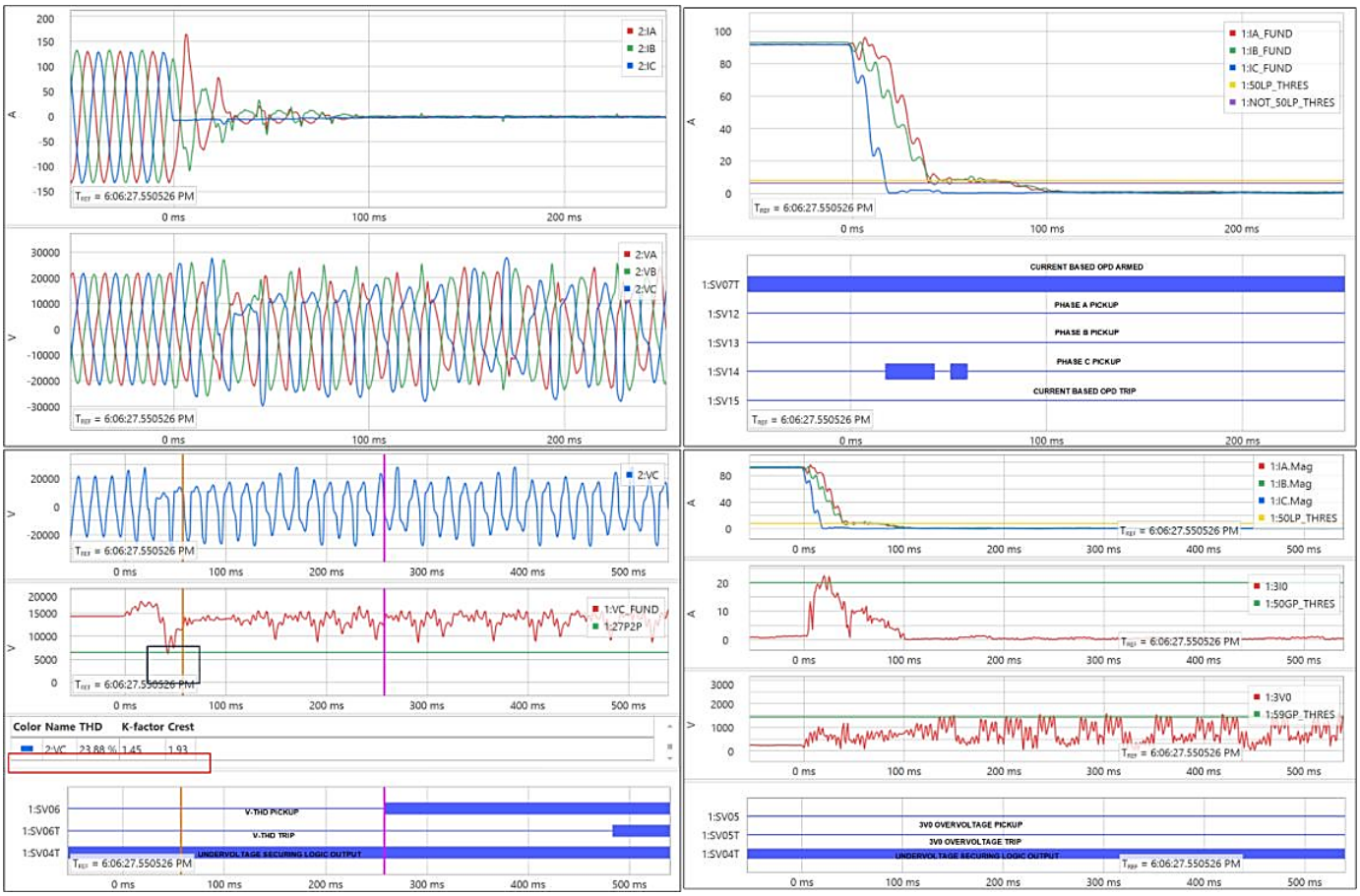

Fig. 13. Site 5 Replay Test Event Report

E. Site 5

Fig. 13 shows an open phase on Phase C on the system side of Recloser R1. The Ip_FUND values show that before the open phase occurred, the filtered current magnitudes on all three phases were higher than the yellow line (50LP_THRES) and this allows the current-based OPD scheme to be armed (SV07T). As the open phase begins, IC_FUND drops below the magenta line (NOT_50LP_THRES), while IA_FUND and IB_FUND remain above the yellow line (50LP_THRES). This results in the current-based OPD scheme picking up (SV14), but it does so only briefly, hence there is not enough time to trip on this current-based OPD scheme (SV15). IA_FUND and IB_FUND fall below the yellow line soon after, which causes SV14 to deassert approximately 0.017 seconds later. It can be observed, from the raw current waveforms (Ip), that the DER output current collapses on all three phases in less than 0.100 seconds.

Such high-speed shutdown of DER output current in response to an open phase on the system-side of the PCC recloser has also been observed on other sites and associated events. In such cases, current-based OPD is not feasible.

To detect this open phase, voltage-based OPD schemes are relied upon. As mentioned before, the voltage-based OPD scheme described in Section IV is employed in the OPD device along with the current-based schemes. Voltage-based OPD consists of a zero-sequence overvoltage scheme and a total harmonic distortion scheme, as shown in Fig. 2 and Fig. 3 respectively. Fig. 12 shows that the zero-sequence voltage (3V0) is less than the green line (59GP_THRES), and is not enough to detect this open-phase fault.

Fig. 12 shows the total harmonic distortion measured on Phase-C voltage. The event analysis software was used to measure the THD of the selected signal over a 0.2 second averaging window between the orange (left) cursor and the magenta (right) cursor. This calculation results in a value of 21.07 percent, which is above the threshold setting of 7.5 percent. The voltage THD-based OPD scheme picks up (SV06) and trips (SV06T) about 0.5 seconds after the open-phase fault begins.

The V-THD-based OPD scheme uses the output of the undervoltage-securing logic (SV04T) for supervision, as shown in Fig. 3. In this event, the ferroresonance condition caused oscillations in the calculation of the magnitude, as shown by VC_FUND. There are also a few instances in this event where VC_FUND drops below the 27P1P threshold (one such instance is highlighted with a black box), thereby dropping the input to the undervoltage-securing logic, SV04. A one-cycle dropout time was added to the SV04 timer, which allowed the output of the undervoltage securing logic (SV04T) to ride through possible oscillations in Vp_FUND magnitude. Note that [1] and [12] did not include this dropout time; and it was an enhancement added for occurrences like displayed in Fig. 13.

Section II and IV provide all the recommended set points for the OPD schemes used in this paper.

F. Summary of Field Events

The field events presented in this section show that current-based OPD schemes are effective in fast detection and clearing of open-phase events, as long as there is a sufficient amount of output current from the DER, thereby allowing the current-based OPD schemes to be armed.

It is important to note that the effectiveness of any current-based OPD scheme depends on the ability of the DER to maintain current injection into the open-phase fault for longer than the time required to qualify a trip of this scheme.

In some cases, the DER output currents shut down extremely quickly, and there is not enough time for the current-based OPD schemes to pick up or trip. This is significant in cases like Site 5, where the current-based OPD scheme fails to trip as the DER output current shuts down in less than 0.1 second.

For such cases, the voltage-based OPD schemes remain dependable. To maintain reliability—regardless of the output current of the DER, the response time of the DER for external open-phase faults, or the transformer connection type—a combination of current- and voltage-based OPD schemes is proposed, as described in Section IV.

Table II shows the performance of all OPD schemes for the five events reviewed in this section.

TABLE II
PERFORMANCE OF OPD SCHEMES FOR FIELD EVENTS

Site	1	2	3	4	5
Load Level (% of Capacity)	17.71%	86.39%	25.96%	86.26%	51.33%
Current	True	True	True	True	False
Maximum 3V0	0.68 pu	0.17 pu	0.25 pu	0.68 pu	0.06 pu
3V0 Overvoltage	True	True	True	True	False
Maximum Voltage THD	9.31%	74.89%	2.74%	22.39%	21.05%
V-THD Scheme	True	True	False	True	True

VII. MODELING IN RTDS

The test system shown in Fig. 8 was modeled in the RTDS test environment to validate the current-based OPD scheme. The inverter was integrated to the RTDS distribution circuit model using a manufacturer-provided black-box model configured with field parameters via the Giga-Transceiver System-on-a-Chip module. The voltage and current signals from the R1 recloser control were applied to the OPD device under test using the low-level test interface via the RTDS Giga-Transceiver Analog Output card.

The generator step-up (GSU) transformer was modeled using the unified magnetic equivalent circuit model where the high-side and low-side connections and core construction were varied, as shown in Table III. The inverter loading was tested between 5 and 90 percent. A single open-phase event was simulated between R1 and R2 on the high side of the GSU transformer for each testing permutation.

TABLE III
RTDS TESTING MATRIX OF THE CURRENT-BASED OPD SCHEME

XFMR	Core Construction	Loading	SV15
Dyn11	3-/5-Limb	5–90%	X
YNd10	3-/5-Limb	5–90%	X
Dy11	3-/5-Limb	5–90%	X
Yd1	3-/5-Limb	5–90%	X
YNy0	3-/5-Limb	5–90%	X
Yyn0	3-/5-Limb	5–90%	X
Yy0	3-/5-Limb	5–90%	X
Dd0	3-/5-Limb	5–90%	X

Fig. 14 shows an open Phase-B event on a 3-limb YNd1 transformer under 90 percent loading. SV13 asserted upon detection of the open phase event and stayed asserted until the current-based OPD algorithm timed-out (SV15).

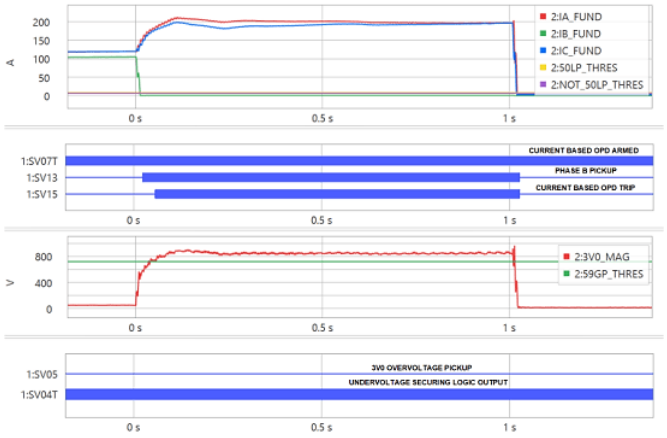

Fig. 14. Open Phase-B Event on a 3-Limb YNd1 Transformer Under 90% Loading

In this event, the inverter shut down after one second because of the overvoltage condition caused by the open phase. It should be noted that the zero-sequence voltage was above the 59G1 pickup (59GP_THRES), but the 3V0 overvoltage OPD was blocked from operation because the current on the healthy phases was above the 50LP set point while the inverter was online. Once the inverter shut down, the zero-sequence voltage went away because the voltage was fully reconstructed on the opened phase as a result of the transformer configuration.

Fig. 15 shows an open Phase-B event on a 5-limb Yd1 transformer under 90 percent loading. SV13 asserted upon detection of the open-phase event and stayed asserted until the current-based OPD algorithm timed-out (SV15).

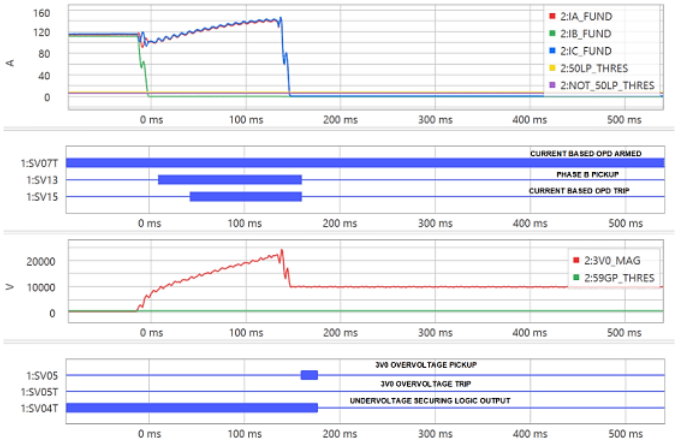

Fig. 15. Open Phase-B Event on a 5-Limb Yd1 Transformer Under 90% Loading

However, the inverter shut down after ten cycles because of the overvoltage condition caused by the open phase. It should be noted that the zero-sequence voltage was above the 59G1 pickup (59GP_THRES), but the 3V0 overvoltage OPD was prevented from operation because the current on the healthy phases was above the 50LP set point while the inverter was online. Once the inverter shut down, the voltage on the opened phase dropped to 0.4 pu keeping the zero-sequence voltage above the 59G1 pickup; however, it was restrained from operation in this case because the voltage on the opened phase was below the 27P2P set point, causing the voltage securing logic output (SV04T) to drop out. For this event, IEEE 1547 Undervoltage Level 2 (UV2) protection, commonly available at the PCC, is expected to trip the PCC breaker in two seconds as a backup to the current-based OPD scheme. These tests were repeated for another plant that has a system topology similar to the one shown in Fig. 8 using the same inverter manufacturer, with the main difference being the inverter configuration parameters. Fig. 16 shows an open Phase-B event on a 3-limb Dy11 transformer under 90 percent loading.

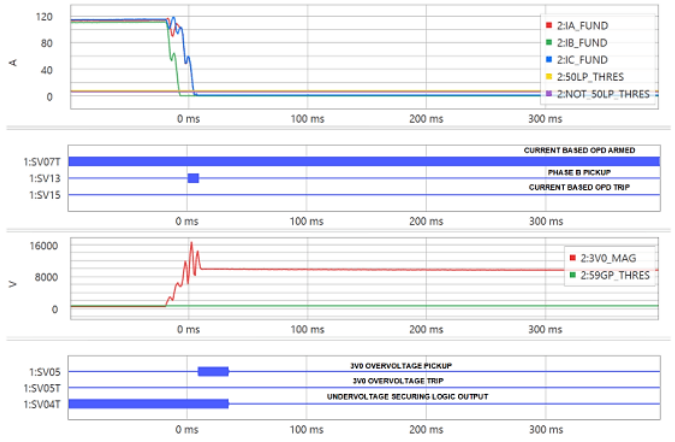

Fig. 16. Open Phase-B Event on a 3-limb Dy11 Transformer Under 90% Loading.

In this case, the current-based OPD algorithm detected the open phase (SV13); however, the inverter shut down before it could time out (SV15). This was because the inverter was configured to trip in one cycle if the voltage exceeded 1.3 pu at this plant. The voltage on the open phase dropped to 0.4 pu once the inverter shut down, at which point the IEEE 1547 UV2 protection was expected to trip the PCC breaker in under two seconds. This behavior occurred at this site on ungrounded GSU transformers at higher loading levels where the voltage was not fully reconstructed after the inverter shutdown, requiring no additional algorithm changes to address this response.

In summary, the RTDS testing showed that the current-based OPD algorithm correctly detected the open-phase events irrespective of transformer connection, core construction, or loading level (5–90 percent).

VIII. RMS Current-Based OPD Scheme

In the events presented in Section V, the DER output currents are heavily distorted during an open-phase fault on the utility side of the PCC. For this reason, a rms current-based OPD scheme was considered and evaluated, as the rms method of estimating analog signal magnitude provides a higher output as compared to the cosine filter for waveforms with harmonic distortion. This higher magnitude could increase the sensitivity of current-based OPD at light loading levels, as it would be easier to detect current on the unfaulted phases.

The OPD device used in this paper provides an averaging filter with a 12-cycle (for 60 Hz systems) update rate to measure rms quantities. This long averaging window was found to be too slow for current-based OPD.

To compare the performance of using rms currents as opposed to fundamental currents for OPD, a one-cycle rms filter was built in the event analysis software and applied to the field-event reports. Analysis of these events showed that while this rms filter performed to satisfaction, there was no significant advantage in using rms current magnitudes over fundamental current magnitudes for OPD.

IX. Conclusion

This paper proposes using voltage- and current-based schemes for OPD at the PCC. As discussed in Sections II and V, the OPD schemes are supervised by the current flow at the PCC. Fig. 17 summarizes the availability of these schemes at various levels of current flow at the PCC, represented as a percentage of DER-rated output.

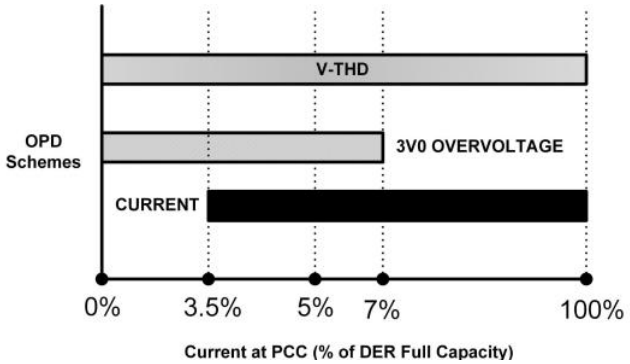

Fig. 17. Availability of OPD Schemes Based on Current at PCC

The current-based OPD scheme is available if there is enough current (as qualified by the 50LP threshold) at the PCC to arm this scheme. Field-event replay testing and an inverter-based DER manufacturer-provided black-box model testing in the RTDS environment demonstrate that the current-based OPD scheme is reliable when the inverter-based DER is exporting at least five percent rated current, independent of interconnection transformer winding connection, core construction, and grounding.

In cases where the open phase occurs when the current-based OPD is not armed, voltage-based OPD is relied upon to trip the PCC breaker. The proposed combination of the current and zero-sequence overvoltage-based OPD scheme provides overlap of coverage when current flow at PCC is at five percent of inverter-based DER-rated output (or the minimum current rating of the DER, if that is higher), which satisfies the open-phase detection-type test requirement defined by IEEE 1547.1.

In some cases, (where the current-based OPD scheme is armed when the open phase occurs) this scheme may fail to detect the open phase if the inverter-based DER output shuts down too quickly, as observed in Section VI. However, this DER shutdown allows the zero-sequence overvoltage OPD scheme to be unblocked, as the current at PCC falls below the supervision threshold. This scheme is now available to detect the open phase, as demonstrated in Section V1.B.

In some cases, the voltage on the open phase drops below 0.4 pu, which causes the voltage-based OPD to be blocked. However, the PCC breaker is tripped in under two seconds by the definite time 27 element that is typically implemented at the PCC to comply with the abnormal voltage DER response requirement in IEEE 1547.

In some cases, partial reconstruction of the lost phase voltage by the interconnection transformer with certain connection types and core configurations limits the dependability of the zero-sequence overvoltage OPD scheme. This effect is most prominent when the transformer is at no load or is very lightly loaded [8] [9] [13].

This means that when DER is offline or is operating at very low capacity, both the current-based OPD scheme and the zero-sequence overvoltage OPD scheme may lose dependability. Fig. 18 shows the availability of voltage-based OPD schemes and IEEE 1547 UV2 protection, based on the reconstructed voltage measured on the open phase.

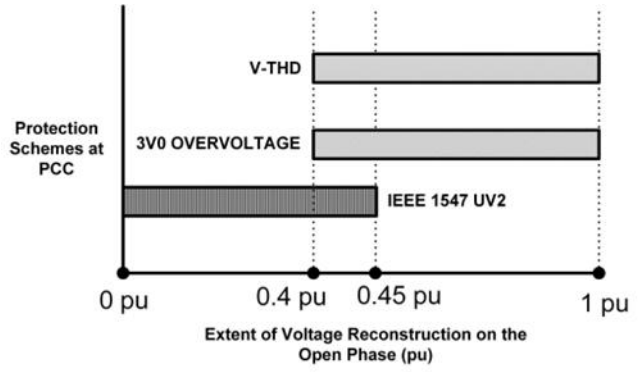

Fig. 18. Availability of Voltage-Based OPD Schemes and IEEE 1547 UV2 Protection at PCC.

The V-THD OPD scheme is available immediately after the open phase occurs, as demonstrated in Section VI.E. There is no known gap in the dependability of this scheme based on current flow at PCC, or based on the interconnection transformer configuration or core construction. However, this scheme is not 100 percent dependable in every application, as explained in Section III. The combination of all three OPD schemes provides extremely high reliability of open-phase detection at the PCC.

X. Appendix

TABLE IV
SETTING RECOMMENDATIONS FOR VOLTAGE- AND CURRENT-BASEDOPD SCHEMES

Element	Units	Settings Recommendations [1] [12]
27P1P	Volts	Set to Level 1 undervoltage pickup of the PCC relay
27P2P	Volts	Set to 90% of the level 2 undervoltage pickup of the PCC relay (the setting must be less than 27P1P)
59GP	Volts	The default setting is 10% of the nominal voltage
50GP	Amperes	Set less than the ground fault pickup of the PCC relay
V-THDP	Percent	The default setting is 7.5%
50LP	Amperes	Set less than 5% of inverter-based DER-rated output current (See Equation 1)
SV04PU	Seconds	The default setting is 1 second
SV04DO	Seconds	The default setting is 0.017 seconds (~one cycle at 60 Hz)
SV05PU	Seconds	The default setting is 0.083 seconds (~five cycles at 60 Hz)
SV05DO	Seconds	The default setting is 0 seconds
SV06PU	Seconds	Set between 0.22–1.8 seconds
SV06DO	Seconds	The default setting is 0 seconds
SV07PU	Seconds	The default setting is 0.5 seconds (30 cycles at 60 Hz)
SV07DO	Seconds	The default setting is 2 seconds
SV12PU SV13PU SV14PU	Seconds	Set greater than or equal to 0.03 seconds (~2 cycles)
SV12DO SV13DO SV14DO	Seconds	Default setting is 0 seconds

XI. References

[1] J. Gahan, A. Valdez, B. Cockerham, R. Chowdhury, and J. Town, "Field Experience With Open-Phase Testing at Sites With Inverter-Based Resources," proceedings of the 74th Annual Conference for Protective Relay Engineers, College Station, TX, March 2021.

[2] *IEEE Standard for Interconnection and Interoperability of Distributed Energy Resources with Associated Electric Power Systems Interfaces*, IEEE Standard 1547, 2018.

[3] X. Shi, T. Key, W. Wang, and A. Huque, "Detection of Feeder Open Phase Events Using Smart Inverters," presented at the 2020 47th IEEE Photovoltaic Specialists Conference (PVSC), Virtual, Jun. 15–Aug. 21, 2020.

[4] *IEEE Standard Conformance Test Procedures for Equipment Interconnecting Distributed Energy Resources with Electric Power Systems and Associated Interfaces*, IEEE Standard 1547.1, 2020.

[5] "Nuclear Maintenance Application Center: Development and Analysis of an Open Phase Detection Scheme for Various Configurations of Auxiliary Transformers," EPRI Technical Report, 2013.

[6] M. Rusicior, J. Young, and A. Burfield, "Open-Phase Detection in the SEL-751 and SEL-751A Feeder Protection Relays," SEL Application Guide Voume III AG2016-07, 2016.

[7] R. Chowdhury, N. Fisher, "Transmission Line Protection for Systems With Inverter-Based Resources—Part I: Problems," *IEEE Transactions on Power Delivery*, Vol. 36, No. 4, August 2021.

[8] M. Ropp, D. Schutz, S. Perlenfein, and C. Mouw, "Single-Phase Open Detection in the Presence of Distributed Energy Resources," proceedings of the 44th Western Protective Relay Conference, Spokane, WA, 2017.

[9] A. Abd-Elkader, H. Chaluvadi, "Open-Phase Detection for Station Auxiliary Transformers," proceedings of the 45th Annual Western Protective Relay Conference, Spokane, WA, October 2018.

[10] "Methods for Analyzing and Detecting an Open Phase Condition of a Power Circuit to a Nuclear Plant Station Service or Startup Transformer," PES-TR75, January 2020.

[11] S. Uddin, A. Bapary, M. Thompson, R. McDaniel and K. Salunkhe "Application Considerations for Protecting Transformers With Dual Breaker Terminals," proceedings of the 45th Annual Western Protective Relay Conference, Spokane, WA, October 2018.

[12] B. Cockerham, R. Chowdhury, J. Town, and J. Subbarayan, "Open-Phase Detection for Inverter-Based Distributed Energy Resources Using the SEL-735 Meter," SEL Application Guide, Volume V, AG2022-08, 2022.

[13] "Interim Report: EPRI Open-Phase Detection Method," EPRI Technical Report, 2014.

XII. Biographies

Brett Cockerham, PE, earned his BS in electrical engineering technology, summa cum laude, in 2014 and his MSc in applied energy and electromechanical systems in 2016. Both degrees were awarded by the University of North Carolina at Charlotte. In 2014, Brett joined Schweitzer Engineering Laboratories, Inc., (SEL), as an application engineer focusing on power system protection and control. In 2023, Brett joined Burns and McDonnell as a senior electrical engineer with responsibilities in performing coordination studies, protective relay settings and logic, event analysis, and relay testing. Brett has two patents and he has authored more than 18 industry papers, including technical papers and guides, centering around power system protection and metering applications. Brett is a registered professional engineer in the state of North Carolina and a senior member of IEEE.

Joseph Miller earned his BS in electrical engineering in 2021 from Iowa State University. Joseph is currently pursuing his ME in electrical engineering from the University of Idaho. In 2021, Joseph joined Burns & McDonnell as a substation design engineer developing construction drawings and performing studies for substation projects ranging from 34.5 kV to 230 kV. In 2022, Joseph transitioned roles within Burns & McDonnell to a protection engineer with responsibilities including specifying relaying requirements and developing relay settings. Joseph's research interests are in power system protection, control, and automation.

Jai Subbarayan graduated from the National Institute of Technology, Tiruchirappalli, India, in 2016 with a Bachelor of Technology in electrical and electronics engineering with honors, following which he worked for the Dow Chemical Company as an electrical engineer. Jai graduated from North Carolina State University with an MSc in electric power systems engineering in 2019 and joined Schweitzer Engineering Laboratories, Inc., (SEL), as a protection application engineer. Jai supports SEL customers in Florida with protection and metering applications. Jai has authored six papers, including application guides and technical papers in the area of power system protection and metering, and has one patent.

Ahmed Abd-Elkader received his BS in electrical engineering, with honors, from Ain Shams University, Cairo, Egypt, in 2008, an MBA, with honors, from Wake Forest University in Winston-Salem, NC, in 2015, and an MSEE from the University of North Carolina at Charlotte (UNCC), in 2024. He is currently pursuing a PhD in electrical engineering from UNCC. Ahmed is a senior engineer with Schweitzer Engineering Laboratories, Inc., (SEL) with over 16 years of experience in power systems protection and control.